Frequency Domain Estimation of 3-D Rigid Motion Based on Range and Intensity Data

L. Lucchese G. Doretto G. M. Cortelazzo
Department of Electronics and Informatics
University of Padova
Via Gradenigo 6/A, 35131, Padova, Italy
{lulaluc,doretto,corte}@dei.unipd.it

Abstract

Video-rate registered range and intensity data are at reach of current sensor technology. This wealth of data can be profitably exploited in order to estimate rigid motion parameters as the approaches to 3-D motion estimation, based on the optical flow of both types of data, indicate.
This work introduces an alternative for 3-D motion estimation based on the Fourier transform of the 3-D intensity function implicitly described by the registered time-sequences of range and intensity data. The proposed procedure can lead to an unsupervised method for 3-D rigid motion estimation. This method has several advantages related to the fact that it uses the total available information and not sets of features. With respect to memory occupancy the use of a time-sequence of a 3-D intensity function represents a considerable data reduction with respect to a pair of time-sequences of 2-D functions. The proposed technique, which extends to the 3-D case previous frequency domain estimation algorithms developed for the planar case, retain their robustness.

1 Introduction and problem statement

Current sensor technology is able to supply real-time sequences of registered image and intensity data [1, 2]. This wealth of data can be profitably exploited in order to estimate motion parameters as the methods of [3, 4] indicate.
This work proposes an original frequency domain technique for estimating the 3-D rigid motion parameters with a number of potentially interesting characteristics. This method does not use features but the whole information given by a 3-D textured surface to which the data are equivalent. The use of a 3-D textured surface is memory-wise more efficient than using a 2-D textured image jointly with a 2-D range data image. Furthermore the fact that this method is not based on features leaves open the possibility of using simplified structure models. The use of the whole available information makes this procedure very robust, a property tipical of the 2-D motion estimation techniques based on frequency domain [5, 6]. Let $\ell_1(\mathbf{x})$, $\mathbf{x} \in I\!R^3$, be a 3-D object and let $\ell_2(\mathbf{x})$, be a rigidly translated and rotated version of $\ell_1(\mathbf{x})$ (these data can be obtained from registered range and intensity data captured at different times). It can be shown that, without lack of generality, $\ell_1(\mathbf{x})$ and $\ell_2(\mathbf{x})$ relate as

$$\ell_2(\mathbf{x}) = \ell_1(R^{-1}\mathbf{x} - \mathbf{t}) \tag{1}$$

According to (1) $\ell_2(\mathbf{x})$ is first translated by the vector $\mathbf{t} \in I\!R^3$ and then rotated by the matrix[1] $R \in SO(3)$. Denote as

$$\begin{aligned} \mathcal{L}_i(\mathbf{k}) &\doteq \mathcal{F}[\ell_i(\mathbf{x}) \mid \mathbf{k}] = \\ &= \iiint_{-\infty}^{+\infty} \ell_i(\mathbf{x}) e^{-j\,2\pi \mathbf{k}^T \mathbf{x}} d\mathbf{x} \end{aligned} \tag{2}$$

the 3-D cartesian Fourier transform of $\ell_i(\mathbf{x}), i = 1, 2$; it is straightforward to prove that the two transforms are related as

$$\mathcal{L}_2(\mathbf{k}) = \mathcal{L}_1(R^{-1}\mathbf{k}) e^{-j\,2\pi \mathbf{k}^T R \mathbf{t}} \tag{3}$$

Relationships (1) and (3) hold for 3-D surfaces as well as for 3-D solids. However, if the 3-D surfaces were modeled by impulsive functions supported on them, their Fourier transforms should have lot of spurious high frequency content not suited to the frequency domain techniques to be presented. For this reason we preliminarily build 3-D solids from the range data defined by the 3-D surfaces and we apply the proposed technique to them. Texture information is only used

[1] $SO(3) = \{R \in I\!R^{3\times 3}, R^{-1} = R^T, \det(R) = +1\}$ is the group of the 3×3 special orthogonal matrices.

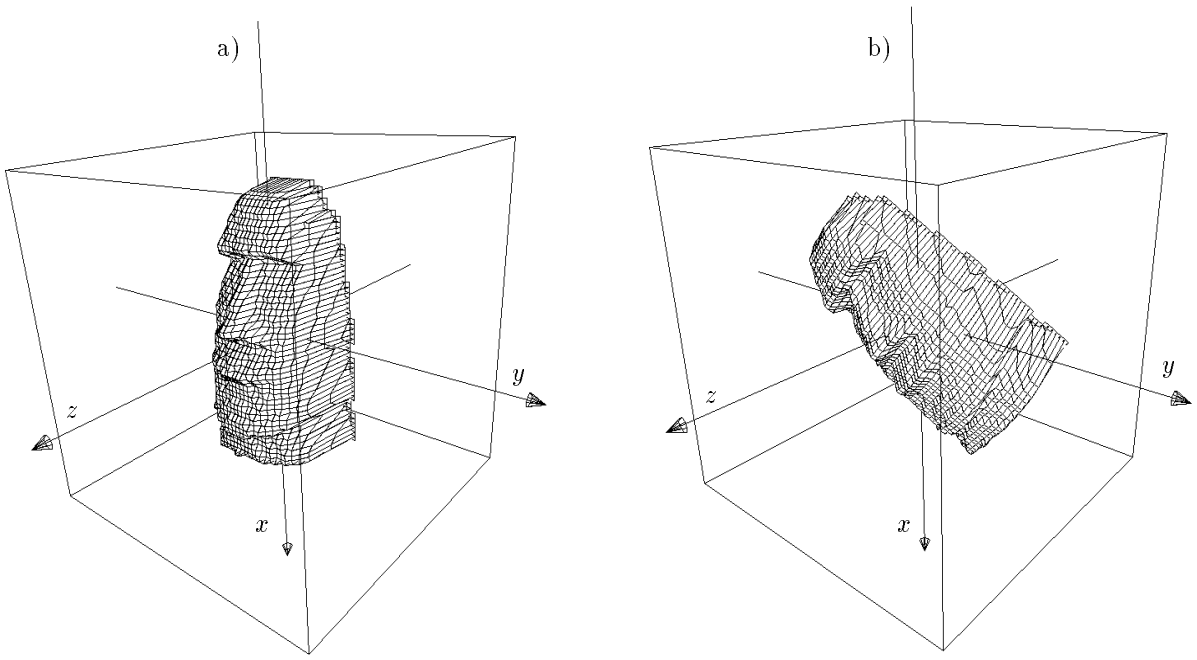

Figure 1: Mohai's head [7]: a) $\ell_1(\mathbf{x})$; b) $\ell_2(\mathbf{x})$.

at the last step of the proposed procedure in order to disambiguate among possible estimates obtained from range data only.

Let $S_1(\mathbf{x})$ and $S_2(\mathbf{x})$, $\mathbf{x} \in I\!R^3$, be the range data defining the surfaces of a rigid body moving in $I\!R^3$, at times t_1 and t_2 respectively. From $S_1(\mathbf{x})$ and $S_2(\mathbf{x})$ define $\ell_1(\mathbf{x})$ and $\ell_2(\mathbf{x})$ as

$$\ell_i(\mathbf{x}) = \begin{cases} 1 & \text{if } \mathbf{x} \in \text{Int}(S_i(\mathbf{x})) \\ 0 & \text{elsewhere} \end{cases} \qquad i = 1, 2 \tag{4}$$

where $\text{Int}(S_i(\mathbf{x}))$ denotes the interior of the surface $S_i(\mathbf{x})$. For example's sake, Fig.1.a as $\ell_1(\mathbf{x})$ shows a Mohai's head from [7], and Fig.1.b shows $\ell_2(\mathbf{x})$ obtained rotating the Mohai's head around the origin.

From (3) one sees that the translational vector $\mathbf{t}$ affects only phases and not magnitudes. Magnitudes are related as

$$|\mathcal{L}_2(\mathbf{k})| = |\mathcal{L}_1(R^{-1}\mathbf{k})| \tag{5}$$

Relationship (5) can be used in order to determine R. Therefore in the frequency domain the estimation of R and $\mathbf{t}$ can be decoupled and one can estimate first R from (5) and then $\mathbf{t}$ from (3).

In order to stress in R the contribution of the rotational axis versor $\omega^T = (\omega_x, \omega_y, \omega_z) \in I\!R^3$, $||\omega|| = 1$, and of the rotational angle $\psi \in I\!R$, let's write R as [8]

$$R = R(\widehat{\omega}, \psi) = e^{\widehat{\omega}\psi} \tag{6}$$

where[2]

$$\widehat{\omega} = \begin{bmatrix} 0 & -\omega_z & \omega_y \\ \omega_z & 0 & -\omega_x \\ -\omega_y & \omega_x & 0 \end{bmatrix} \in so(3) \tag{7}$$

is a skew-symmetric matrix built form the versor ω.

The proposed procedure has three steps: in the first it estimates the rotational axis ω, in the second the rotational angle ψ, in the third the translational vector $\mathbf{t}$.

2 Proposed Technique

2.1 Estimation of the rotational axis

Define the difference function $\Delta(\mathbf{k})$ between the transforms magnitudes as

$$\begin{aligned} \Delta(\mathbf{k}) &= \Delta(k_x, k_y, k_z) \doteq \left| \frac{|\mathcal{L}_1(\mathbf{k})|}{\mathcal{L}_1(\mathbf{0})} - \frac{|\mathcal{L}_2(\mathbf{k})|}{\mathcal{L}_2(\mathbf{0})} \right| = \\ &= \left| \frac{|\mathcal{L}_1(\mathbf{k})|}{\mathcal{L}_1(\mathbf{0})} - \frac{|\mathcal{L}_1(R^{-1}\mathbf{k})|}{\mathcal{L}_1(\mathbf{0})} \right| \end{aligned} \tag{8}$$

where relationship (5) has been used. From (8) it is clear that $\Delta(\mathbf{k}) = 0$ if $R^{-1}\mathbf{k} = \mathbf{k}$ which is equivalent to $R\mathbf{k} = \mathbf{k}$. It can be proved [8] that R, as rotational

[2] $so(3) \doteq \{S \in I\!R^{3\times 3} : S^T = -S\}$ is the space over reals of the 3×3 skew-symmetric matrices. The map $so(3) \to SO(3)$ is suriective [8].

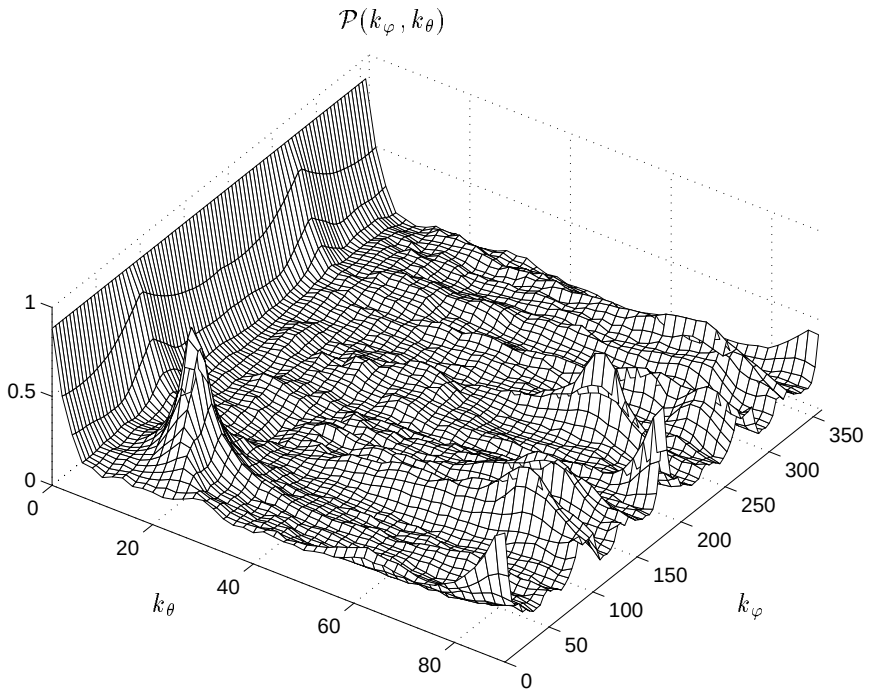

Figure 2: Function $\mathcal{P}(k_\varphi, k_\theta)$ relative to the Mohai's head of Fig.1.

matrix, has eigenvalues $\lambda_1 = 1$, $\lambda_2 = e^{j\psi}$ and $\lambda_3 = e^{-j\psi}$, and that ω has the following properties:

a) it is the eigenvector associated to $\lambda_1 = 1$ (therefore it satisfies $R\mathbf{k} = \mathbf{k}$);

b) it is the only real eigenvector of R.

In other words the locus $\Delta(\mathbf{k}) = 0$ includes a line through ω. For objects without special symmetries (as natural objects typically are) this property of the function $\Delta(\mathbf{k})$ can be exploited in order to determine the versor ω by the following procedure:

i) express $\Delta(k_x, k_y, k_z)$ in spherical coordinates

$$\begin{cases} k_\rho = \sqrt{k_x^2 + k_y^2 + k_z^2} & k_\rho \geq 0 \\ k_\varphi = \arctan \frac{k_y}{k_x} & 0 \leq k_\varphi < 2\pi \\ k_\theta = \arccos \frac{k_z}{\sqrt{k_x^2+k_y^2+k_z^2}} & 0 \leq k_\theta < \pi \end{cases} \quad (9)$$

as $\overline{\Delta}(k_\rho, k_\varphi, k_\theta)$; notice that this function can be represented only in a hemisphere because of the hermitian symmetry of the Fourier transform;

ii) compute the radial projection of $\overline{\Delta}(k_\rho, k_\varphi, k_\theta)$ as

$$\mathcal{P}(k_\varphi, k_\theta) \doteq \int_0^\infty \overline{\Delta}(k_\rho, k_\varphi, k_\theta)\, dk_\rho \quad (10)$$

iii) the angular coordinates of ω in spherical representation (see Fig.3) can be found as

$$(\varphi, \theta) = \arg \min_{k_\varphi, k_\theta} [\mathcal{P}(k_\varphi, k_\theta)] \quad (11)$$

since, from the inclusion of ω within the locus $\Delta(\mathbf{k}) = 0$, $\mathcal{P}(k_\varphi, k_\theta) \geq 0$ with $\mathcal{P}(\varphi, \theta) = 0$;

iv) define ω the versor of the direction (φ, θ).

The use of radial projections (10) simplifies the 3-D search for a line of the locus $\Delta(\mathbf{k}) = 0$ into the minimization of a 2-D function which can be solved by standard numerical methods. Fig.2 shows the function $\mathcal{P}(k_\varphi, k_\theta)$ relative to the Mohai's head example of Fig.1.

2.2 Estimation of the rotational angle

Once the rotational axis ω ha been determined, the estimate of the rotational angle ψ can be conveniently approached in a cartesian coordinate system with an axis along ω, as shown in Fig.3. The determination of this coordinate system and the representation in this system of relationship (5) between magnitudes can be obtained as follows. Define the cartesian coordinates system

$$\mathbf{u} \doteq \begin{bmatrix} u \\ v \\ w \end{bmatrix} = \mathcal{C}^T \begin{bmatrix} k_x \\ k_y \\ k_z \end{bmatrix} \quad (12)$$

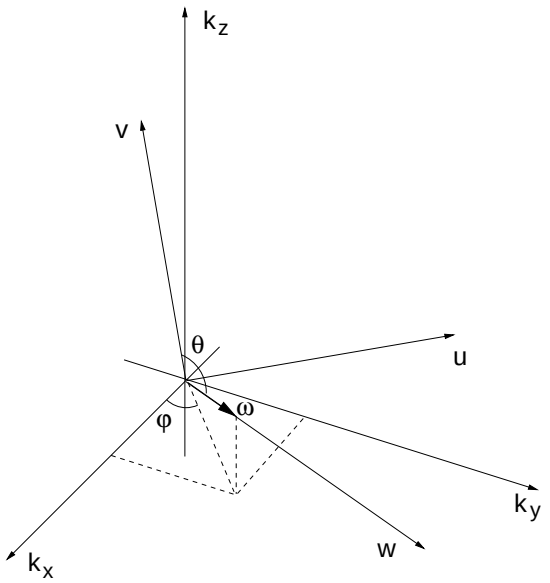

Figure 3: Change of coordinate reference systems.

with[3]

$$\mathcal{C} = \begin{bmatrix} -\sin\varphi & -\cos\theta\cos\varphi & \sin\theta\cos\varphi \\ \cos\varphi & -\cos\theta\sin\varphi & \sin\theta\sin\varphi \\ 0 & \sin\theta & \cos\theta \end{bmatrix} \qquad (13)$$

In the new cartesian reference system defined through (12) and (13) equation (5) becomes

$$|\mathcal{L}_2(\mathcal{C}\mathbf{u})| = |\mathcal{L}_1(R^{-1}\mathcal{C}\mathbf{u})| = |\mathcal{L}_1(\mathcal{C}\mathcal{C}^{-1}R^{-1}\mathcal{C}\mathbf{u})| \quad (14)$$

Define for convenience $|\bar{\mathcal{L}}_i(\mathbf{u})| \doteq |\mathcal{L}_i(\mathcal{C}\mathbf{u})|$, $i = 1, 2$, from which (14) can be written as

$$|\bar{\mathcal{L}}_2(\mathbf{u})| = |\mathcal{L}_1(\mathcal{C}^{-1}R^{-1}\mathcal{C}\mathbf{u})| = |\mathcal{L}_1(R_w^{-1}(\psi)\mathbf{u})| \quad (15)$$

where

$$R_w(\psi) = \mathcal{C}^{-1}R\mathcal{C} = \begin{bmatrix} \cos\psi & -\sin\psi & 0 \\ \sin\psi & \cos\psi & 0 \\ 0 & 0 & 1 \end{bmatrix} \doteq \doteq \left[\begin{array}{cc|c} & & 0 \\ & r(\psi) & 0 \\ \hline 0 & 0 & 1 \end{array}\right] \qquad (16)$$

Matrix $R_w(\psi)$ clearly shows the structure of a rotation by ψ around the w-axis. Note that sub-matrix $r(\psi)$ is a 2-D rotational matrix, i.e. $r(\psi) \in SO(2)$. If the magnitudes (15) are projected along the w-axis as

$$p_i(u, v) = \int_{-\infty}^{+\infty} |\bar{\mathcal{L}}_i(u, v, w)| dw \qquad i = 1, 2 \qquad (17)$$

[3] $\mathcal{C} \in SO(3)$ and then $\mathcal{C}^{-1} = \mathcal{C}^T$.

given the structure of $R_w(\psi)$, it is easy to prove that the axial projections defined in (17) relate as

$$p_2\left(\begin{bmatrix} u \\ v \end{bmatrix}\right) = p_1\left(r^{-1}(\psi)\begin{bmatrix} u \\ v \end{bmatrix}\right) \qquad (18)$$

Fig.4 shows axial projections $p_1(u, v)$ and $p_2(u, v)$ relative to the Mohai's head of Fig.1. The determination of ψ from (18) is a planar rotational problem which can be solved as follows. Define the polar reference system (r, α) related to the cartesian system (u, v) as $r = \sqrt{u^2 + v^2}$, $\alpha = \arctan(v/u)$ and define $\bar{p}_i(r, \alpha) \doteq p_i(r\cos\alpha, r\sin\alpha), i = 1, 2$. Compute the 1-D radial projections of $\bar{p}_i(r, \alpha)$, $i = 1, 2$, as

$$f_i(\alpha) = \int_0^{\infty} \bar{p}_i(r, \alpha) dr \qquad i = 1, 2 \qquad (19)$$

It can be easily shown [6] that $f_2(\alpha)$ is related to $f_1(\alpha)$ as

$$f_2(\alpha) = f_1(\alpha - \psi) \qquad (20)$$

i.e. that the two functions differ only in a phase shift ψ. Fig.5 shows $f_1(\alpha)$ and $f_2(\alpha)$ relative to the Mohai's head of Fig.1. Projections are again used in order to reduce the dimensionality of the problem by one. Furthermore by means of (19), the original 2-D problem of estimating the rotational angle ψ is turned into the problem of estimating a 1-D translational shift (of value ψ). This 1-D problem can be solved by 1-D phase-correlation [9] as follows. Denote the Fourier transform of functions $f_i(\alpha), i = 1, 2$, as

$$F_i(k_\alpha) \doteq \mathcal{F}[f_i(\alpha) \mid k_\alpha] = \int_0^{\pi} f_i(\alpha) e^{-j\,2\pi k_\alpha \alpha} d\alpha \quad (21)$$

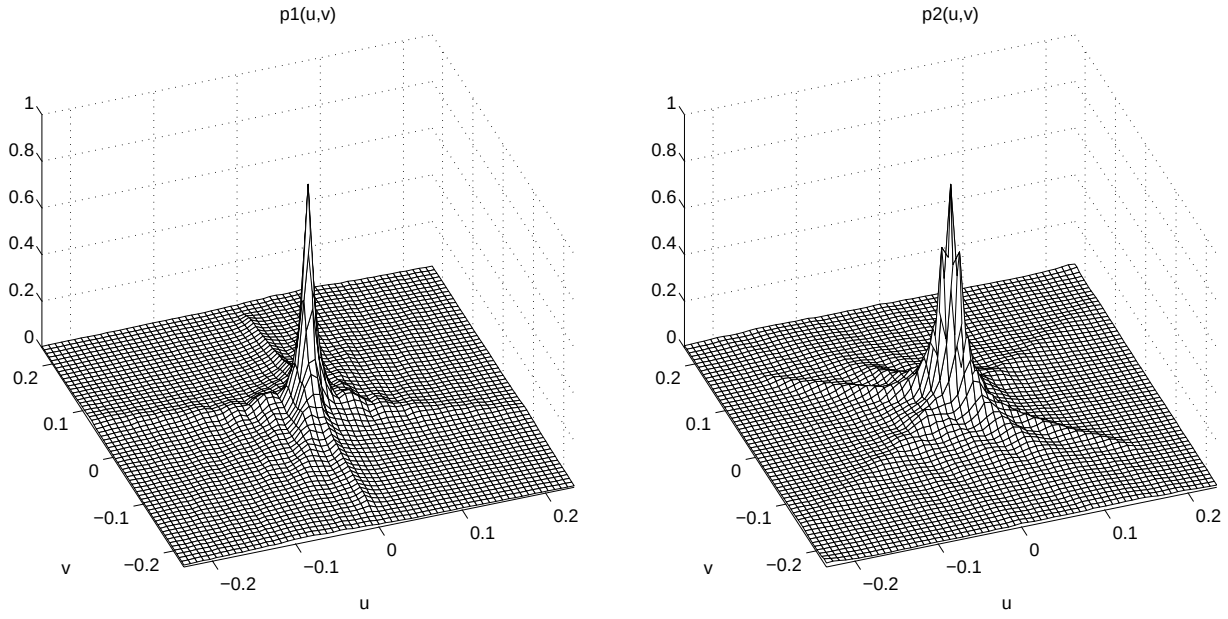

Figure 4: Axial projections $p_1(u,v)$ and $p_2(u,v)$.

from (20) it is readly seen that

$$F_2(k_\alpha) = F_1(k_\alpha) e^{-j\,2\pi k_\alpha \psi} \tag{22}$$

From the normalized product

$$\Gamma(k_\alpha) \doteq \frac{F_1^*(k_\alpha) F_2(k_\alpha)}{F_1(k_\alpha) F_2(k_\alpha)} = e^{-j\,2\pi k_\alpha \psi} \tag{23}$$

one can compute the so called phase correlation function

$$\gamma(\alpha) \doteq \mathcal{F}^{-1}[\Gamma(k_\alpha) \mid \alpha] = \delta(\alpha - \psi) \tag{24}$$

which is the inverse Fourier transform of (23). The peak of $\gamma(\alpha)$, which in practice is not strictly impulsive, gives nevertheless an estimate of ψ, denoted as $\widehat{\psi}$, (see [6] for the details). Phase correlation function $\gamma(\alpha)$ relative to $f_1(\alpha)$ and $f_2(\alpha)$ is shown in Fig.5. Phase correlation gives as equally likely estimates $\widehat{\psi}$ and $\widehat{\psi} + \pi$. In order to disambiguate the estimate one can use texture information. In our simulations we mapped arbitrary texture on the Mohai's head, which in [7] is given only as range data, in order to have registered range and intensity data. Fig.6 (top row) shows the superposition of $f_1(\alpha)$ and $g_2(\alpha) \doteq f_2(\alpha + \widehat{\psi})$. The accuracy of the match is remarkable as evidenced by the error $e(\alpha) \doteq f_1(\alpha) - g_2(\alpha)$ shown in Fig.6 (bottom row).
From ω and ψ the rotational matrix $R(\widehat{\omega}, \psi)$ can be reconstructed by means of the Rodrigues' formula [8] as

$$R(\widehat{\omega}, \psi) = e^{\widehat{\omega}\psi} = I + \widehat{\omega} \sin\psi + \widehat{\omega}^2 (1 - \cos\psi) \tag{25}$$

In the example of Fig.1, the 3-D rotation in spherical coordinates is defined by parameters $\varphi = 109.5°, \theta = 24.5°$ (which are the coordinates of ω in the spherical coordinate system) and $\psi = 51.5°$; the parameters estimated by the proposed frequency domain technique are $\widehat{\varphi} = 109°, \widehat{\theta} = 24.5°$ and $\widehat{\psi} = 51.5°$. There is only an error in the estimate of φ.

2.3 Estimation of the 3-D translational vector

The translational vector $\mathbf{t}$ can be estimated as follows:

a) de-rotate image $l_2(\mathbf{x})$ as

$$d_2(\mathbf{x}) = l_2(R\mathbf{k}) = l_1(\mathbf{x} - \mathbf{t}) \tag{26}$$

b) apply a 3-D cartesian phase correlation algorithm [9] on $\mathcal{L}_1(\mathbf{k})$ and $\mathcal{D}_2(\mathbf{k}) \doteq \mathcal{F}[d_2(\mathbf{x}) \mid \mathbf{k}] = \mathcal{L}_1(\mathbf{k})\ e^{-j\,2\pi \mathbf{k}^T \mathbf{t}}$, i.e. compute the normalized product between transforms as

$$Q(\mathbf{k}) \doteq \frac{\mathcal{L}_1^*(\mathbf{k}) \mathcal{D}_2(\mathbf{k})}{|\mathcal{L}_1(\mathbf{k}) \mathcal{D}_2(\mathbf{k})|} = e^{-j\,2\pi \mathbf{k}^T \mathbf{t}} \tag{27}$$

c) evaluate its inverse Fourier transform

$$q(\mathbf{x}) \doteq \mathcal{F}^{-1}[Q(\mathbf{k}) \mid \mathbf{x}] = \delta(\mathbf{x} - \mathbf{t}) \tag{28}$$

The translational vector $\mathbf{t}$ can be estimated from the peak of the 3-D impulsive function $q(\mathbf{x})$.

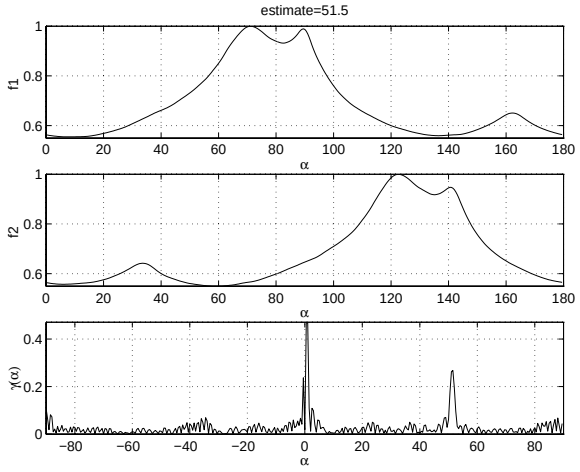

Figure 5: Functions $f_1(\alpha)$ (top row) and $f_2(\alpha)$ (middle row) and phase-correlation $\gamma(\alpha)$ (bottom row).

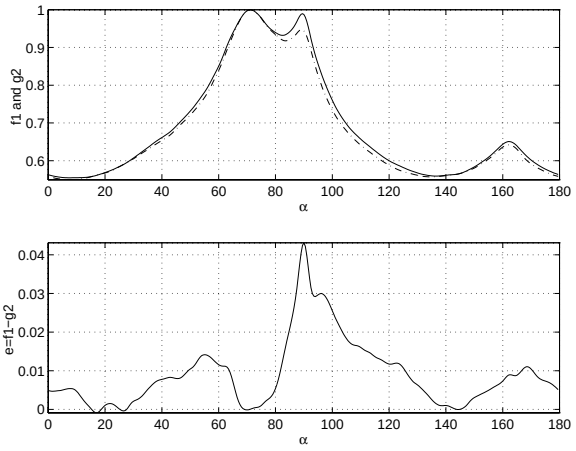

Figure 6: Superposition of $f_1(\alpha)$ (solid line) and $g_2(\alpha)$ (dotted line, top row); error function $e(\alpha) = f_1(\alpha) - g_2(\alpha)$ (bottom row).

Experimental data showing the actual performance of the algorithm will complete the proposed submission. The method can be efficiently implemented by using MD FFT algorithms [10, 11].

3 Conclusions

The presented technique is a method for the non-supervised estimate of the 3-D rigid motion by means of range and intensity data. Its novelty relies upon the fact that it is a frequency domain approach; therefore it uses the global information of the data and not sets of features. This is probably one of the causes of its robustness.

At the time of this writing we are only able to give a progress report on this work and not the final assessment of its performance. For this one needs further experimental work with real data.

Current work also considers an extension of this approach to range data only and its application to the unsupervised registration of range data. Algorithmic refinements of the presented procedure, aimed to enhance its precision and speed, are also under study.

Acknowledgements

Work partially supported under "CNR Progetto Finalizzato Beni Culturali".

References

[1] J.A. Beraldin, F. Blais, M. Rioux, J. Domey and L. Cournoyer, "A Video Rate Laser Range Camera for Electronic Boards Inspection", *Proceedings of Vision 90*, Detroit, MI, Nov. 12-15, 1990.

[2] J.A. Beraldin, F. Blais, M. Rioux, J. Domey and L. Cournoyer, "Registered Range and Intensity at 10-Mega Samples per Second", Opt. Eng., 31(1), 88-94 (1992).

[3] D.H. Ballard and O.A. Kimball, "Rigid Body Motion from Depth and Optical Flow", *Computer, Vision Graphics and Image Processing*, vol. 22, pp. 95-115, 1983.

[4] P. Boulanger and J.A. Beraldin, "Three Dimensional Motion Estimation Using Range and Intensity Flow", NRCC internal report, Ottawa.

[5] L. Lucchese, G.M. Cortelazzo, C. Monti, "A Frequency Domain Technique for Estimating Rigid Planar Rotations", *Proc. of ISCAS'96*, Atlanta, Georgia, May 1996, Vol. 2, pp. 774-777.

[6] L. Lucchese, G.M Cortelazzo, C. Monti, "High Resolution Estimation of Planar Rotations Based on Fourier Transform and Radial Projections", to appear in *Proc. of ISCAS-97*, Hong Kong.

[7] M. Rioux and L. Cournoyer, *The NRCC Three-dimensional Image Data Files*, Ottawa: National Research Council of Canada, June 1988.

[8] R. Murray, Z. Li and S. Sastry, *A Mathematical Introduction to Robotic Manipulation*, CRC Press, 1994.

[9] C.D. Kuglin and D.C. Hines, "The phase correlation image alignement method", *Proc. IEEE 1975 Int. Conf. Cybern. Soc.*, 1975, pp. 163-165.

[10] R. Bernardini, G.M. Cortelazzo, G.A. Mian, "A Sequential Multidimensional Cooley-Tukey Algorithm", *IEEE Trans. Signal Processing*, 42, pp. 2430-2438, Sept. 1994.

[11] R. Bernardini, G.M. Cortelazzo, G.A. Mian, "Unit Radix Graphs and Their Application to the Computation of MD FFT", submitted.